Monthly Notices of the ROYAL ASTRONOMICAL SOCIETY LETTERS

Mon. Not. R. Astron. Soc. **424,** L6–L10 (2012) doi:10.1111/j.1745-3933.2012.01274.x

Typical density profile for warm dark matter haloes

Jordi Viñas,⋆ Eduard Salvador-Solé and Alberto Manrique

Institut de Ciències del Cosmos, Universitat de Barcelona (UB–IEEC), Martí i Franquès 1, E-08028 Barcelona, Spain

Accepted 2012 April 17. Received 2012 April 12; in original form 2012 February 13

ABSTRACT

Using the model for (bottom-up) hierarchical halo growth recently developed by Salvador-Solé et al., we derive the typical spherically averaged density profile for haloes with several relevant masses in the concordant warm dark matter (ΛWDM) cosmology with non-thermal sterile neutrinos of two different masses. The predicted density profiles become flat at small radii, as expected from the effects of the spectrum cut-off. The core cannot be resolved, however, because the non-null particle velocity yields the fragmentation of minimum mass protohaloes in small nodes, which invalidates the model at the corresponding radii.

Key words: galaxies: haloes – cosmology: theory – dark matter.

1 INTRODUCTION

Matter in the Universe is predominantly dark and clustered in haloes that grow through mergers and accretion. The concordant Λ, cold dark matter (CDM), model recovers the observed large-scale properties of the Universe: it correctly predicts the microwave background radiation anisotropies (Komatsu et al. 2011) and galaxy clustering (Cole et al. 2005). However, some problems arise in the small-scale regime: it predicts excessive substructure with a deficient distribution of maximum circular velocities (Klypin et al. 1999; Moore et al. 1999; Boylan-Kolchin, Bullock & Kaplinghat 2011) and a sharp central cusp in the halo density profile, apparently in conflict with the profiles observed in dwarf galaxies (Goerdt et al. 2006). While the disagreement in the satellite abundance and characteristics might be explained through the inhibition of star formation owing to several baryonic feedback processes, the cusp problem might be insurmountable (but see Governato et al. 2012; Macciò et al. 2012a).

Several modifications of the ΛCDM model have been proposed that, keeping its right predictions at large scales, may improve those compromised at small scales. This includes the cosmological models dominated by self-interacting dark matter (Bento, Bertolami & Rosenfeld 2000; Kaplinghat, Knox & Turner 2000; Spergel & Steinhart 2000) and dissipationless collisionless warm dark matter (WDM). The best candidate particles in the latter category of dark matter are the gravitino (Ellis et al. 1984; Hogan & Dalcanton 2000; Kaplinghat 2005; Gorbunov, Khmelnitsky & Rubakov 2008) and non-thermal sterile neutrino (Dodelson & Widrow 1994; Hogan & Dalcanton 2000; Shaposhnikov & Tkachev 2006). Specifically, the case of light sterile neutrinos is being attracting growing interest as these kinds of particles are naturally foreseen in a minimal extension of the standard model.

⋆E-mail: jvinas@am.ub.es

The non-negligible WDM particle velocities at decoupling introduce a cut-off in the power spectrum due to free streaming and, at the same time, a bound in the fine-grained phase-space density. The former effect should inhibit the formation of haloes below the corresponding free-streaming mass scale, $M_{\rm fs}$. Thus, if the cusp in CDM haloes arises from very low mass, extremely concentrated, halo ancestors, the absence of haloes with masses below $M_{\rm fs}$ would translate into the formation of a core. The latter effect should give rise to an upper bound in the coarse-grained phase-space density of haloes resulting from virialization, which could also lead to a non-divergent central density profile. Both aspects depend, however, critically on the poorly known way haloes fix their density profiles.

In fact, *N*-body simulations do not seem to confirm such expectations: WDM haloes show similar density profiles as CDM haloes (e.g. Colombi, Dodelson & Widrow 1996; Colín, Avila-Reese & Valenzuela 2000; Knebe et al. 2002; Wang & White 2009; Schneider et al. 2011). Only a small hint towards increased scaled radii has been found (Bode, Ostriker & Turok 2001), although the opposite trend, namely a slight inflection towards sharper density profile at small radii (∼0.02–0.03 times the virial radius $R_{\rm vir}$), has also been reported (Colín, Valenzuela & Avila-Reese 2008). A core has only been found in the recent work by Macciò et al. (2012b). The situation is further complicated by the fact that simulations of WDM cosmologies find a substantial amount of haloes with masses considerably smaller than $M_{\rm fs}$. These low-mass haloes are spurious due to the periodical grid used in simulations (Wang & White 2007), but even so they could affect the density profile of more massive haloes formed from their mergers and accretion. In addition, the expected size of the core (if any) for the relevant WDM particle masses is close to the resolution of current simulations, which might explain the negative results above.

All these uncertainties would disappear if the halo density profile could be inferred analytically down to arbitrarily small radii directly from the power spectrum of density perturbations. Salvador-Solé et al. (2012, hereafter SVMS) have recently built a model for the

inner structure of dissipationless collisionless dark matter haloes in (bottom-up) hierarchical cosmologies[1] that fills this gap.

In this Letter, we apply the SVMS model to the ΛWDM cosmology with 2-keV thermalized and non-thermalized sterile neutrinos. The linear power spectrum in WDM cosmologies endowed with non-thermal sterile neutrinos with mass m_ν is given by (Viel et al. 2005)

$$P_{\rm WDM}(k) = T_{\rm fs}^2(k) P_{\rm CDM}(k), \tag{1}$$

where $P_{\rm CDM}(k)$ is the power spectrum for the ΛCDM cosmology, given here by the 7-year *Wilkinson Microwave Anisotropy Probe* (*WMAP*7) concordance model (Komatsu et al. 2011), and $T_{\rm fs}(k)$ is the 'transfer' function, well fitted by

$$T_{\rm fs}(k) = [1 + (\alpha k)^{2\mu}]^{-5/\mu}\,, \tag{2}$$

with $\mu = 1.12$ and

$$\alpha = 0.1655 \left(\frac{h}{0.7}\right)^{0.22} \left(\frac{m_\nu}{1\,{\rm keV}}\right)^{-0.136} \left(\frac{\Omega_{\rm WDM}}{0.228}\right)^{0.692} {\rm Mpc}, \tag{3}$$

here h being the current value of the Hubble parameter in units of $100\,{\rm Mpc}^{-1}\,{\rm km\,s}^{-1}$, and $\Omega_{\rm WDM}$. The spectrum for fully thermalized particles with mass $m_{\rm WDM}$ is essentially equal to that for non-thermalized particles with mass m_ν given by (Viel et al. 2005)

$$m_\nu = 4.286 \left(\frac{m_{\rm WDM}}{1\,{\rm keV}}\right)^{4/3} \left(\frac{h}{0.7}\right)^{-2/3} \left(\frac{\Omega_{\rm WDM}}{0.273}\right)^{-1/3} {\rm keV}. \tag{4}$$

Therefore, the case of thermalized sterile neutrinos with $m_{\rm WDM} = 2\,{\rm keV}$ is equivalent to that of non-thermalized ones with $m_\nu = 10.8\,{\rm keV}$. The two masses, $m_\nu = 10.8$ and 2 keV here considered, yield (equation 3) $\alpha = 0.032$ and 0.151 Mpc, respectively. We remind that $m_\nu = 10.8\,{\rm keV}$ (or $m_{\rm WDM} = 2$) sterile neutrinos are compatible with observational constraints such as the Lyα forest and the abundance of Milky Way satellites, while the case of lower particle masses is unclear (e.g. Boyarsky et al. 2009; Polisensky & Ricotti 2011).

2 THE MODEL

In any *bottom-up hierarchical cosmology*, haloes form through either major mergers or smooth accretion (including minor mergers). Both processes involve the virialization of the halo each time the mass increases. As virialization is a relaxation process yielding the memory loss of the past history, the density profile for haloes having suffered major mergers is indistinguishable from that for haloes having grown by pure accretion (PA; see SVMS for a complete rigorous explanation). Consequently, we have the right to concentrate in the latter kind of haloes.

As shown in SVMS, *accreting dissipationless collisionless dark matter haloes* evolve from the inside out, keeping their instantaneous inner structure unaltered. In these conditions, the radius of the sphere with mass M is exactly given by

$$r(M) = \frac{3GM^2}{10\,|E_{\rm p}(M)|}, \tag{5}$$

where $E_{\rm p}(M)$ is the total energy of the sphere encompassing the same mass M in the (spherically averaged) seed, namely a peak in the primordial random Gaussian density field filtered at the scale M. Thus, provided the energy distribution in peaks is known, equation (5) is an implicit equation for the halo mass profile $M(r)$.

We must remark that equation (5) is only valid provided that the isodensity contours in the seed reach turnaround without shell-crossing at increasingly larger radii (see SVMS). This is certainly the case when the initial peculiar velocities are negligible, as those induced by random Gaussian density fluctuations, and the seed expands in linear regime. However, if there are peculiar velocities of non-gravitational origin such that they dominate the dynamics at small enough scales, then the system may not expand in linear regime and there may be shell-crossing before turnaround, so equation (5) may no more be valid. We will come back to this possibility in Section 4.

In the parametric form, $E_{\rm p}(M)$ is given by the total energy in the sphere with radius $R_{\rm p}$ centred at the peak,

$$E_{\rm p}(R_{\rm p}) = 4\pi \int_0^{R_{\rm p}} {\rm d}r_{\rm p}\, r_{\rm p}^2\, \langle\rho_{\rm p}\rangle(r_{\rm p}) \times \left\{ \frac{[H(t_{\rm i}) r_{\rm p} - v_{\rm p}(r_{\rm p})]^2}{2} + \frac{\sigma_{\rm DM}^2(t_{\rm i})}{2} - \frac{GM(r_{\rm p})}{r_{\rm p}} \right\}, \tag{6}$$

together with the mass of the sphere,

$$M = 4\pi \int_0^{R_{\rm p}} {\rm d}r_{\rm p}\, r_{\rm p}^2\, \langle\rho_{\rm p}\rangle(r_{\rm p})\,, \tag{7}$$

where $\langle\rho_{\rm p}\rangle(r_{\rm p})$ is the spherically averaged (unconvolved) protohalo density profile, $M(r_{\rm p})$ is the corresponding mass profile, $H(t_{\rm i})$ is the Hubble parameter at the cosmic time $t_{\rm i}$ when the seed is considered, $\sigma_{\rm DM}(t_{\rm i})$ is the adiabatically evolved particle velocity dispersion of non-gravitational origin[2] and $v(r_{\rm p})$ is, to leading order in the deviations from spherical symmetry, the peculiar velocity at the radius $r_{\rm p}$ in the seed owing to the inner mass excess,[3]

$$v_{\rm p}(r_{\rm p}) = -\frac{2G\left[M(r_{\rm p}) - 4\pi r_{\rm p}^3 \bar\rho(t_{\rm i})/3\right]}{3H(t_{\rm i}) r_{\rm p}^2}, \tag{8}$$

$\bar\rho(t_{\rm i})$ being the mean cosmic density at $t_{\rm i}$.

The steps to be followed are thus the following: (1) determination of the spherically averaged protohalo density profile $\langle\rho_{\rm p}\rangle(r_{\rm p})$ from the linear power spectrum of the cosmology considered (see Section 3), (2) calculation from it of the energy distribution $E_{\rm p}(M)$ (equations 6 and 7) and (3) derivation of the typical halo mass profile $M(r)$ by inversion of equation (5), and of the typical spherically averaged halo density profile, through the trivial relation

$$\langle\rho\rangle(r) = \frac{1}{4\pi r^2}\frac{{\rm d}M}{{\rm d}r}. \tag{9}$$

3 PROTOHALO DENSITY PROFILE

In PA, every halo ancestor along the continuous series ending at the halo with M at t also arises from one peak in the random density field at $t_{\rm i}$, filtered at the mass scale of the ancestor. Thus, the value at the centre of the protohalo ($r_{\rm p} = 0$) of the convolution of the spherically averaged density contrast profile for the protohalo, $\langle\delta_{\rm p}\rangle(r_{\rm p})$, by a

[1] In WDM cosmologies there is a minimum halo mass, but haloes still form hierarchically through the merger of less massive objects previously formed and their accretion of diffuse matter.

[2] The velocity dispersion due to random density fluctuations is several orders of magnitude smaller and can be safely neglected (see SVMS).

[3] In equation (8) we have taken into account that the cosmic virial factor $f(\Omega) \approx \Omega^{0.1}$ is at $t_{\rm i}$ very approximately equal to one.

Gaussian window of every radius R_f must be equal to the density contrast of the peak (in the density filed equally convolved),

$$\delta_{pk}(R_f) = \frac{4\pi}{(2\pi)^{3/2} {R_f}^3} \int_0^\infty dr_p\, r_p^2\, \delta_p(r_p)\, e^{-\frac{1}{2}\left(\frac{r_p}{R_f}\right)^2}. \quad (10)$$

Therefore, provided that the peak trajectory, $\delta_{pk}(R_f)$, associated with the accreting halo were known, equation (10) could be seen as a Fredholm integral equation of first kind for $\langle\delta_p\rangle(r_p)$. Such an equation can be solved (see SVMS for details), so this would lead to the density profile $\langle\rho_p\rangle(r_p)$ for the seed of the halo evolving by PA.

Furthermore, in any *random Gaussian density field*, the typical peak trajectory $\delta_{pk}(R_f)$ leading to a purely accreting halo with typical density profile is the solution of the differential equation (see SVMS and references therein):

$$\frac{d\delta_{pk}}{dR_f} = -x_e(\delta_{pk}, R_f)\sigma_2(R_f)R_f, \quad (11)$$

where $\sigma_2(R_f)$ is the second-order spectral moment and $x_e(R_f, \delta_{pk})$ is the inverse of the average inverse curvature x (minus the Laplacian over σ_2) of peaks with density contrast δ_{pk} at the scale R_f (see SVMS for the explicit form of these two functions). The quantities $\sigma_2(R_f)$ and $x_e(R_f, \delta_{pk})$ depend on the power spectrum of the particular CDM or WDM cosmology considered, so does also the typical peak trajectory solution of equation (11). This equation can be solved for the boundary condition $\delta_{pk}[R_f(M)] = \delta(t)$ leading to the halo with M at t according to the one-to-one correspondence between peaks and haloes given by Manrique & Salvador-Solé (1995)

$$R_f(M) = \frac{1}{q}\left[\frac{3M}{4\pi\bar{\rho}(t_i)}\right]^{1/3}, \qquad \delta(t) = \delta_c(t)\frac{G(t_i)}{G(t)}, \quad (12)$$

where q is the radius, in units of R_f, of the collapsing cloud with volume equal to $M/\bar{\rho}(t_i)$ associated with the peak, $G(t)$ is the cosmic growth factor and $\delta_c(t)$ is the critical linearly extrapolated density contrast for spherical collapse at t. In the underlying ΛCDM cosmology here considered, such a correspondence is given by $q = 2.75$ and $\delta_c(z) = 1.82 + (6.03 - 0.472z + 0.0545z^2)/(1 + 0.000\,552z^3)$ (SVMS).

The peak trajectories, $\delta_{pk}(R_f)$, solution of equation (11) in the WDM (CDM) cosmology for haloes with several masses, are shown in Fig. 1. As can be seen, the $\delta_{pk}(R_f)$ trajectories in the WDM cosmology level off, contrarily to those in the CDM cosmology, at some value δ_{fs} that depends on the halo mass. The time t_{fs} corresponding to δ_{fs} (equation 12) marks the time when the first ancestor of the halo forms and initiates the continuous series of ancestors leading by PA to that final halo. Before that time there is no ancestor of haloes with that mass in the WDM cosmology. Instead, there are halo ancestors down to any arbitrarily small time in the CDM cosmology, with no spectrum cut-off.

In Fig. 2, we show the spherically averaged density profile, $\langle\rho_p\rangle(r_p)$, of WDM (and CDM) halo seeds resulting from equation (10) for the peak trajectories depicted in Fig. 1. As can be seen, contrarily to their CDM counterparts, the WDM halo seeds show apparent flat cores with a universal mass very approximately equal to the mass $M_{fs} = [4\pi/3]\,\bar{\rho}(t_0)\,(\lambda_{fs}^{eff}/2)^3 = 4.7 \times 10^5\,M_\odot$ ($6.8 \times 10^7\,M_\odot$) for $m_\nu = 10.8$ keV ($m_\nu = 2$ keV) sterile neutrinos associated with the effective free-streaming scale length $\lambda_{fs}^{eff} \equiv 2\pi/k_{fs}^{eff} = \alpha$. Note that this is different from the mass associated with scale length equal to 2π over the wavenumber where $T_{fs}^2(k)$ decreases to 0.5, also often used to estimate the free-streaming mass. This latter scale length is substantially greater than α, so it would correspond to the scale length where the effects of WDM begin to be noticeable rather than the minimum size of density perturbations. For this reason, following Schneider et al. (2011), the mass $\sim 1.8 \times 10^9\,M_\odot$ ($\sim 1.9 \times 10^{11}\,M_\odot$) associated with it will be called the half-mode mass M_{hm}.

If the velocity dispersion in the seed were negligible, its flat core with mass $\sim M_{fs}$ would expand and collapse at once, with no

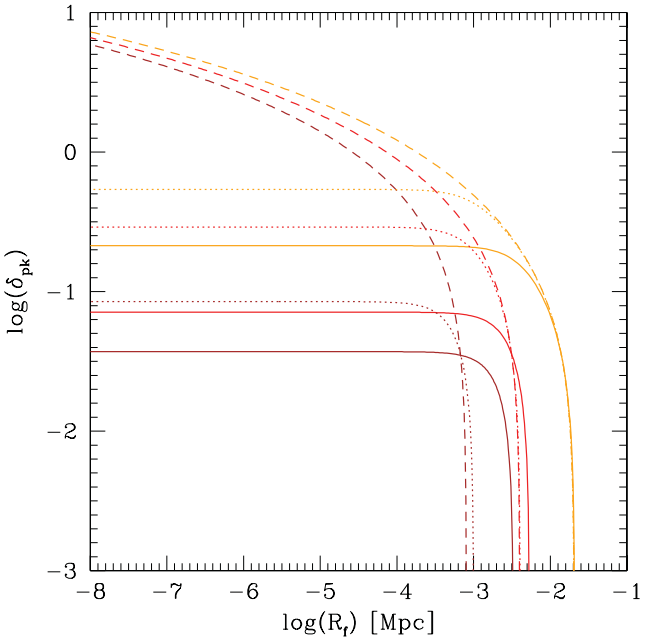

Figure 1. Central density contrast of peaks in the filtered density field at $z = 100$ giving rise by PA to current haloes with masses equal to $10^9\,M_\odot$ (brown lines), $10^{11}\,M_\odot$ (red lines) and $10^{13}\,M_\odot$ (orange lines) as a function of the Gaussian filtering radius R_f. The different curves correspond to the ΛCDM concordance cosmology (dashed lines) and the ΛWDM cosmology with $m_\nu = 2$ keV (solid lines) and $m_\nu = 10.8$ keV (dotted lines) sterile neutrinos. Filtering radii, R_f, are in physical units.

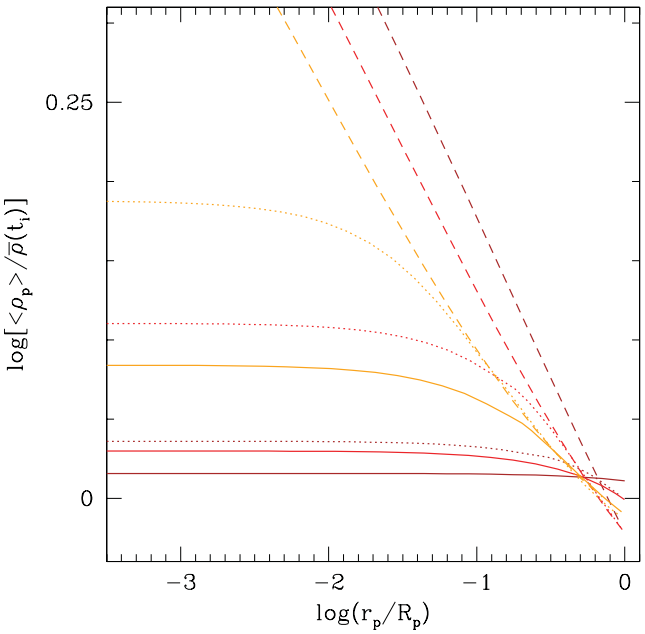

Figure 2. Spherically averaged (unconvolved) density profile for the same halo seeds and cosmologies as in Fig. 1 (same lines).

shell-crossing before turnaround.[4] Consequently, these flat proto-halo cores with mass $\sim M_{\rm fs}$ set a lower bound for the mass of WDM haloes. In contrast, there is no lower bound for the mass of CDM haloes either. One can find ancestors of any accreting halo with M at t down to arbitrarily small cosmic times and with arbitrarily low masses.

4 WDM HALO DENSITY PROFILE

The lower bound mass, $M_{\rm fs}$, for haloes in the WDM cosmology just mentioned arises from the spectrum cut-off. But this bound mass has been obtained by neglecting the WDM particle velocity dispersion, $\sigma_{\rm DM}$. Actually, the non-negligible velocity dispersion of WDM particles causes the total energy $E_{\rm p}(R_{\rm p})$ in the seed (equation 6) to become positive for radii $R_{\rm p}$ below some value of $R_{\rm E}$. This means that shells inside that radius, with velocity dispersion larger than the Hubble velocity, expand more rapidly than outer ones, which causes the system to run out of linear regime, leading to the formation of caustics. These caustics will fragment (owing to the perturbation of the surrounding matter) and give rise to small nodes with masses substantially less than $M_{\rm E} \equiv M(R_{\rm E})$, the mass of that part of the seed with null total energy. This means that haloes with masses below $M_{\rm E} > M_{\rm fs}$ do not actually evolve in the bottom-up fashion and that the typical WDM halo density profile will not satisfy equation (5) at radii enclosing $M_{\rm E}$.

According to Boyanovsky, de Vega & Sanchez (2008), the value of $\sigma_{\rm DM}$ today for non-thermal sterile neutrinos is related to the free-streaming wavenumber through

$$k_{\rm fs}^{\rm eff} \approx \left[\frac{3H^2(t_0)\,\Omega_{\rm M}}{2\sigma_{\rm DM}^2(t_0)}\right]^{1/2}. \qquad (13)$$

In the present case, this leads to $\sigma_{\rm DM}(t_0) = 1.09\,{\rm km\,s^{-1}}$ ($0.23\,{\rm km\,s^{-1}}$). This value is markedly greater than the one usually adopted in such studies, which might overestimate the effects of the velocity dispersion on the predicted structure of WDM haloes. For this reason, we will be more conservative and adopt $\sigma_{\rm DM}(t_0) = 0.075\,{\rm km\,s^{-1}}$. To study the effects of changing the value of $\sigma_{\rm DM}(t_0)$, the density profiles so obtained will be compared to those arising from null $\sigma_{\rm DM}(t_0)$, so as to see the effects of the cut-off in the spectrum alone, as well as from a value of $\sigma_{\rm DM}(t_0)$ equal to that of thermal neutrino-like WDM particles. According to Steffen (2006), this latter velocity dispersion is given by

$$\sigma_{\rm DM}^3(t_0) = 0.042^3 \left(\frac{h}{0.7}\right)^2 \left(\frac{m_\nu}{1\,{\rm keV}}\right)^{-4} \frac{\Omega_{\rm WDM}}{0.273}\,\left({\rm km\,s^{-1}}\right)^3, \qquad (14)$$

leading for $m_\nu = 10.8\,{\rm keV}$ ($m_\nu = 2\,{\rm keV}$) particles to $0.015\,{\rm km\,s^{-1}}$ [$\sigma_{\rm DM}(t_0) = 0.0018\,{\rm km\,s^{-1}}$]. The reference ΛCDM halo profiles are derived assuming a negligible $\sigma_{\rm DM}(t_0)$.

In Fig. 3, we plot the typical spherically averaged halo density profiles for current haloes with the same masses as used in the previous figures, each of them for the three values of $\sigma_{\rm DM}(t_0)$ just mentioned. All the profiles deviate from the corresponding CDM halo profiles in the same monotonous way leading to a flat core with mass $M_{\rm fs}$. However, the only profile that can be strictly traced down to the halo centre is for null velocity dispersion. The remaining profiles [for non-vanishing $\sigma_{\rm DM}(t_0)$] show a sharp upturn to infinity at a small enough radius. This reflects the fact that, for M approaching the value $M_{\rm E}$ where $E_{\rm p}(M)$ vanishes (equation 6), equation (5) is no longer valid. For thermal velocity dispersion, the minimum radius reached essentially coincides with the edge of the flat core, while for larger values of $\sigma_{\rm DM}(t_0)$, it is significantly larger. The mass $M_{\rm E}$ encompassed by the minimum radius reached in the case of non-thermal velocity dispersion shows a slight trend to diminish with increasing halo mass. Specifically, for $m_\nu = 10.8\,{\rm keV}$ ($m_\nu = 2\,{\rm keV}$) and $\sim 0.075\,{\rm km\,s^{-1}}$, it is about $10^9\,{\rm M_\odot}$ ($10^{10}\,{\rm M_\odot}$), $1.8\times10^8\,{\rm M_\odot}$ ($4.6\times10^8\,{\rm M_\odot}$) and $8.1\times10^7\,{\rm M_\odot}$ ($1.2\times10^8\,{\rm M_\odot}$) for haloes with 10^9, 10^{11} and $10^{13}\,{\rm M_\odot}$, respectively. Given the values of $R_{\rm vir}$, respectively, equal to 0.026, 0.12 and 0.57 Mpc, this leads to core radii of about 0.2 kpc (2 kpc), 0.1 kpc (1 kpc) and 0.05 (0.5 kpc), respectively.

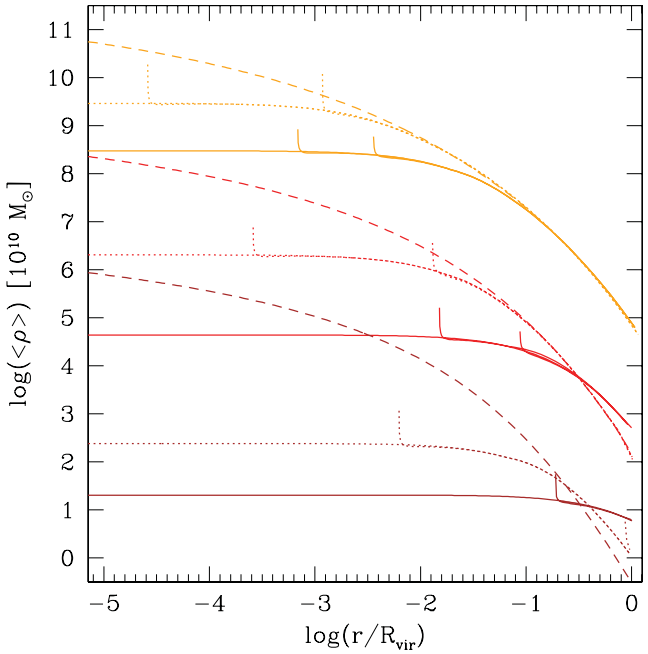

Figure 3. Typical spherically averaged density profiles predicted for the same haloes and in the same cosmologies (same lines) as in previous figures, with null velocity dispersion (curves down to the halo centre), with thermal velocity dispersion (down to the inner break) and with non-thermal velocity dispersion (down to the outer break). To avoid crowding the profiles corresponding to 10^9 and $10^{13}\,{\rm M_\odot}$ have been shifted 2.5 dex downwards and upwards, respectively.

5 CONCLUSIONS

The typical spherically averaged density profile for haloes with masses greater than $M_{\rm fs}$ in the WDM cosmologies can be derived analytically by means of the SVMS model. The density profiles so obtained show a clear flattening relative to the CDM profiles, independent of the particle velocity dispersion, that evolves into a flat core with mass equal to $\sim 4.7\times10^7\,{\rm M_\odot}$ ($4.1\times10^5\,{\rm M_\odot}$) for $m_\nu = 10.8\,{\rm keV}$ ($m_\nu = 2\,{\rm keV}$) sterile neutrinos. This minimum mass agrees with the mass functions derived from WDM models and simulations (e.g. Zavala et al. 2009; Smith & Markovic 2011). For $m_\nu \geq 10.8\,{\rm keV}$, this leads to core radii that are however less than ∼1 kpc as observed in low surface brightness (LSB) galaxies (Kuzio de Naray & Kaufmann 2011; Salucci et al. 2012), in agreement with Macciò et al. (2012b). The right core radii require $m_\nu \lesssim 2\,{\rm keV}$.

[4] In fact, these shells would not cross each other even after turnaround, meaning that such a flat perturbation would oscillate forever and would not virialize. However, the subsequent shells coming from outside the flat core do cross them and the system finally virializes.

The only effect of particle velocities is that they prevent from reaching the flat core. They cause protohaloes to have null total energy within some small radii encompassing the mass $M_{\rm fs}$. This produces caustics as protohaloes expand, leading to their fragmentation into small nodes, which would explain the presence of haloes with masses below $M_{\rm fs}$ in N-body simulations of WDM cosmologies. Consequently, small mass haloes do not develop in the bottom-up fashion and their density profile cannot be recovered by means of the SVMS model. Specifically, for $\sigma_{\rm DM}(t_0) = 0.075\,{\rm km\,s^{-1}}$, the minimum radius that can be reached for $m_\nu = 10.8\,{\rm keV}$ ($m_\nu = 2\,{\rm keV}$) sterile neutrinos is 26 kpc (26 kpc), 1.5 kpc (12 kpc) and 0.7 kpc (2.3 kpc) in haloes with 10^9, 10^{11} and $10^{13}\,{\rm M}_\odot$, respectively. In principle, the density profile inside that radius may not be flat as essentially found with null velocity. However, given the fixed radius and inner mass, it should not be very different either. The results of numerical simulations by Macciò et al. (2012b) confirm such expectations. The 'unresolved region' defines the minimum mass of haloes formed hierarchically in the case of non-null velocity dispersion. It coincides with the mass of the whole halo for objects with $10^9\,{\rm M}_\odot$ ($10^{10}\,{\rm M}_\odot$) in the case of $m_\nu = 10.8\,{\rm keV}$ ($m_\nu = 2\,{\rm keV}$) and $\sigma_{\rm DM}(t_0) \sim 0.075\,{\rm km\,s^{-1}}$; for thermal velocities, it is more than one order of magnitude less. Thus, the minimum mass of haloes grown hierarchically in the case of $m_\nu = 2\,{\rm keV}$ sterile neutrinos leading to cores with the right size is smaller than $10^9\,{\rm M}_\odot$. These results are slightly less restrictive than those found by Macciò et al. (2012b).

ACKNOWLEDGMENTS

This work was supported by the Spanish DGES, AYA2009-12792-C03-01, and the Catalan DIUE, 2009SGR00217. One of us, JV, was beneficiary of a Spanish FPI grant.

REFERENCES

Bento M. C., Bertolami O., Rosenfeld R., 2000, Phys. Rev. D, 62, 041302
Bode P., Ostriker J. P., Turok N., 2001, ApJ, 556, 93
Boyanovsky D., de Vega H. J., Sanchez N. G., 2008, Phys. Rev. D, 78, 063546
Boyarsky A., Lesbourgues J., Ruchayskiy O., Viel M., 2009, Phys. Rev. Lett., 102, 201304
Boylan-Kolchin M., Bullock J. S., Kaplinghat M., 2011, MNRAS, 415, L40
Cole S. et al., 2005, MNRAS, 362, 505
Colín P., Avila Reese V., Valenzuela O., 2000, ApJ, 539, 561
Colín P., Valenzuela O., Avila Reese V., 2008, ApJ, 673, 203
Colombi S., Dodelson S., Widrow L. M., 1996, ApJ, 458, 1
Dodelson S., Widrow L. M., 1994, Phys. Rev. Lett., 72, 17
Ellis J., Hagelin J. S., Nanopoulos D. V., Olive K., Srednicki M., 1984, Nuclear Phys. B, 238, 453
Goerdt T., Moore B., Read J. I., Stadel J., Zemp M., 2006, MNRAS, 368, 1073
Gorbunov D., Khmelnitsky A., Rubakov V., 2008, J. High Energy Phys., 12, 55
Governato F. et al., 2012, MNRAS, 422, 1231
Hogan C. J., Dalcanton J. J., 2000, Phys. Rev. D, 42, 3329
Kaplinghat M., 2005, Phys. Rev. D, 72, 063511
Kaplinghat M., Knox L., Turner M. S., 2000, Phys. Rev. Lett., 85, 3335
Klypin A. A., Kravtsov A. V., Valenzuela O., Prada F., 1999, ApJ, 522, 82
Knebe A., Devriendt J., Mahmood A., Silk J., 2002, MNRAS, 329, 813
Komatsu E. et al., 2011, ApJS, 192, 18
Kuzio de Naray R., Kaufmann T., 2011, MNRAS, 414, 3617
Macciò A. V., Paduroiu S., Anderhalden D., Schneider A., Moore B., 2012, MNRAS, in press (arXiv:1202.1282)
Macciò A. V., Stinson G., Brook C. B., Wadsley J., Couchman H. M. P., Shen S., Gibson B. K., Quinn T., 2012, ApJ, 744, L9
Manrique A., Salvador-Solé E., 1995, ApJ, 453, 6
Moore B. F., Ghigna S., Governato F., Lake G., Quinn T., Stadel J., 1999, ApJ, 524, L19
Polisensky E., Ricotti M., 2011, Phys. Rev. D, 83, 043506
Salucci P., Wilkinson M. I., Walker M. G., Gilmore G. F., Grebel E. K., Koch A., Frigerio Martins C., Wyse R. F. G., 2012, MNRAS, 420, 2034
Salvador-Solé E., Viñas J., Manrique A., Serra S., 2012, MNRAS, in press (SVMS)
Schneider A., Smith R. E., Maccio A. V., Moore B., 2011, MNRAS, in press (arXiv:1112.0330)
Shaposhnikov M., Tkachev I., 2006, Phys. Lett. B, 639, 414
Smith R. E., Markovic K., 2011, Phys. Rev. D, 84, 063507
Spergel D. N., Steinhart P. J., 2000, Phys. Rev. Lett., 84, 3760
Steffen F. D., 2006, J. Cosmol. Astropart. Phys., 9, 1
Viel M., Lesbourgues J., Haehnelt M. G., Matarrese S., Riotto A., 2005, Phys. Rev. D, 71, 063534
Wang J., White S. D. M., 2007, MNRAS, 380, 93
Wang J., White S. D. M., 2009, MNRAS, 396, 709
Zavala J. , Ying Y. P., Faltenbacher A., Yepes G., Hoffman Y., Gottlöber S., Catinella B., 2009, ApJ, 700, 1779

This paper has been typeset from a TEX/LATEX file prepared by the author.